A Platinum Open Access Journal for Organic Chemistry

Paper

Free to Authors and Readers

DOAJ Seal

Arkivoc **2025** (5) 202512441

Optimization and continuous flow synthesis of felodipine

Thanh Ngoc Nguyen[1*], Tan Minh Vu[1], Nhung Hong Thi Le[1], Hung Quang Tran[2], and Anh Quoc Ngo[2]

[1]*Faculty of Chemical Technology, Hanoi University of Industry, Bac Tu Liem District, Hanoi 10000, Vietnam*
[2]*Institute of Chemistry, Vietnam Academy of Science and Technology, 18 Hoang Quoc Viet, Cau Giay District, Hanoi 10000, Vietnam*
Email: thanhnn@haui.edu.vn

Received 07-18-2025 **Accepted** 09-30-2025 **Published on line** 10-07-2025

Abstract

Continuous flow processes have emerged as an effective strategy for the synthesis of active pharmaceutical ingredients (APIs), offering advantages such as improved heat and mass transfer, better safety, enhanced scalability, and the potential for in-line monitoring. In this study, we present the synthesis of felodipine in a perfluoroalkoxy (PFA) microreactor system. A comprehensive optimization was conducted, exploring the influence of reaction process design, solvents, temperatures, nitrogen sources, catalysts, flow rates, and molar ratios on the reaction outcomes. Under optimized conditions, felodipine was obtained in high selectivity via a one-step flow process, yielding up to 59.2% (HPLC) and 40.1% isolated yield. This efficient and scalable method offers potential applicability for the synthesis of felodipine.

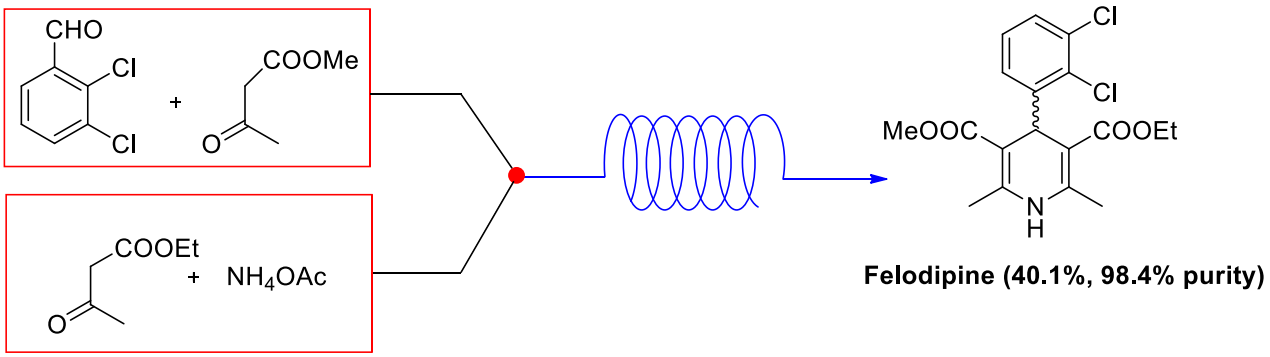

Felodipine (40.1%, 98.4% purity)

Keywords: Felodipine; continuous flow; PFA tubing, 2,3-dichlorobenzylidene acetoacetate, methyl 3-amino crotonate

Cite as *Arkivoc* **2025** (5) 202512441
DOI: https://doi.org/10.24820/ark.5550190.p012.441

Introduction

Felodipine, chemically designated as (*RS*)-3-ethyl 5-methyl 4-(2,3-dichlorophenyl)-2,6-dimethyl-1,4-dihydropyridine-3,5-dicarboxylate, is a long-acting calcium channel blocker widely employed in the treatment of angina pectoris and hypertension.[1-5] Its vasodilatory activity results from the suppression of calcium influx into vascular smooth muscle cells. In addition to its primary action on *L*-type calcium channels, felodipine also binds to other protein–calcium complexes that compete with mineralocorticoid receptors, leading to inhibition of nucleotide phosphodiesterase activity and further modulation of calcium-dependent pathways.[6-8] The industrial synthesis of felodipine typically follows a two-step sequence[9-13]: a Knoevenagel condensation between 2,3-dichlorobenzaldehyde and methyl acetoacetate, followed by a Hantzsch-type cyclization with ethyl 3-aminocrotonate. Conventional methods often require hazardous catalysts such as pyridine and involve labor-intensive operations.

To improve the manufacturing process, the chemical industry has started to embrace more advantageous emerging technologies, particularly continuous flow chemistry. This approach enables many improvements to be performed to the manufacturing process, as previously described in academic literature.[14-19]. Hence, implementing a felodipine manufacturing procedure is imperative to enhance process stability, optimize production, and allow manipulation in industrial manufacturing and applications. Simultaneously, the procedure necessitates a substantial product yield, high purity, simplified operation, and practicality. In this paper, we report our findings on the development of an efficient and safer method for the synthesis of felodipine using a continuous flow process.

Results and Discussion

The synthesis of felodipine by the continuous flow method is shown in Scheme 1:

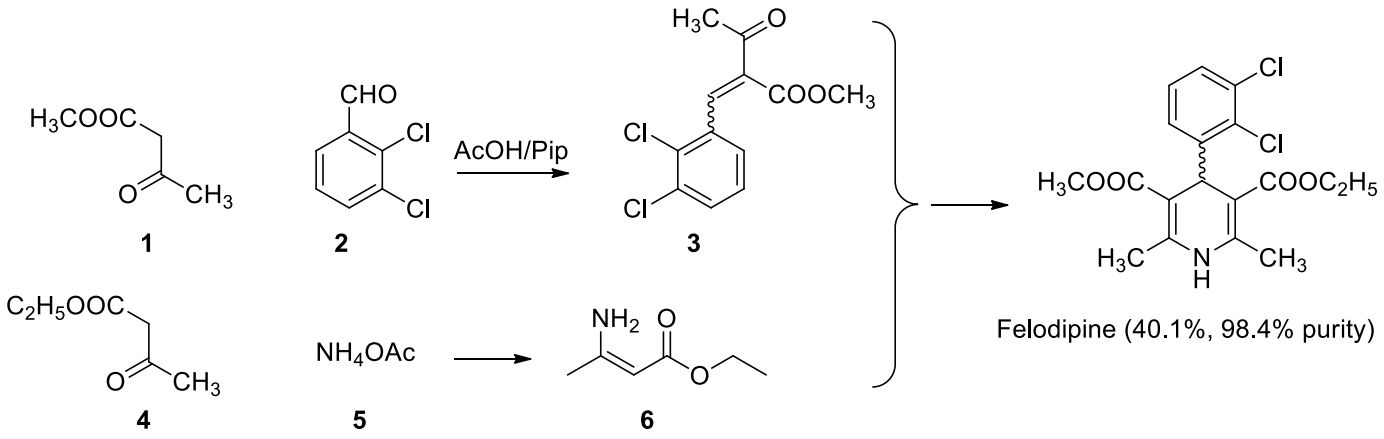

Scheme 1. Continuous flow synthesis of felodipine.

The mechanistic pathway for the continuous-flow synthesis of felodipine can be rationalized in three steps. In the first step, the aldehyde **2** undergoes condensation with methyl acetoacetate **1** to furnish intermediate **3.** In the second step, ammonia, generated in situ from ammonium acetate **5**, reacts with ethyl

acetoacetate **4** to provide intermediate **6**. In the final stage, intermediates **3** and **6** undergo a concerted Hantzsch-type cyclization, in which new C–C and C–N bonds are formed simultaneously, ultimately affording felodipine as the target dihydropyridine product. This mechanistic rationale is consistent with classical reports on multicomponent Hantzsch reactions and their modern adaptations in flow chemistry (Scheme 2).[20]

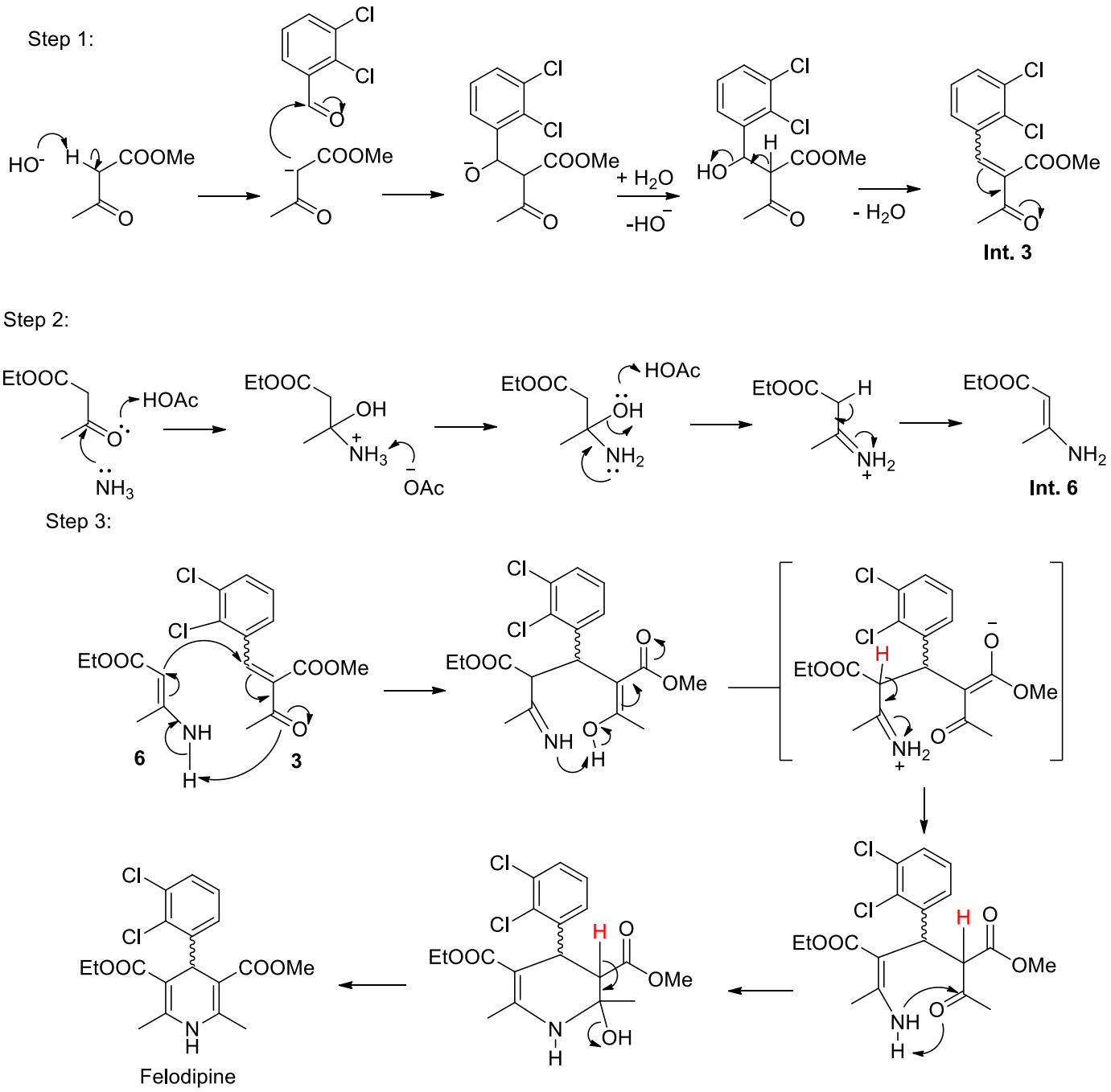

Scheme 2. Proposed mechanistic pathway for the continuous-flow synthesis of felodipine: Step 1 – formation of intermediate **3**; Step 2 – formation of intermediate **6**; Step 3 – final cyclization leading to felodipine.

Although the reaction pathway is intrinsically selective, competing side reactions often reduce the purity and isolated yield of felodipine. Two-step methods that aim to isolate intermediates or modify the catalytic system have shown limited success and often rely on toxic, expensive, or environmentally hazardous reagents.

To address these limitations, we implemented a continuous flow strategy, which allows for precise control of reaction variables, minimizes intermediate accumulation, and provides consistent residence time. This approach enhances chemoselectivity and reproducibility while offering scalability suitable for industrial applications.[16,17] The continuous flow synthesis of felodipine was systematically optimized in two major phases:

Phase I – Optimization of Core Reaction Conditions: Key parameters —including process configuration (single- or two-stage setup), solvent, temperature, and nitrogen source — were systematically optimized to enhance conversion and selectivity (see Table 1).

Phase II – Catalyst, Stoichiometry, and Flow Optimization: The catalytic system, reagent ratios, and flow parameters were fine-tuned to improve throughput, maximize efficiency, and ensure stable operation under continuous conditions (see Table 2*).*

This two-pronged strategy enabled the identification of optimal continuous flow conditions, significantly improving the synthetic yield and purity of felodipine while reducing the formation of by-products. The methodology offers a scalable, cleaner, and more sustainable route for felodipine synthesis compared to conventional batch processes.

1. Optimization of core reaction conditions

Reaction process design. Three reaction configurations (Processes **A**–**C**) were evaluated under identical conditions—total flow rate of 200 µL/min (100 µL/min per channel), 40 °C, acetic acid/pyridine catalyst system, and 10 min residence time—to identify an efficient flow protocol for felodipine synthesis. The corresponding HPLC chromatograms are shown in Figure 1 **1a**–**c**, confirming the retention time of felodipine at 3.23 min across all processes.

Process **A** (Sequential: **1** + **2** → **4** + **5**): Condensation of compounds **1** and 2 was carried out in channel A; the resulting intermediate was then merged with ethyl acetoacetate (**4**) and ammonium acetate (**5**) in channel B. This approach afforded the highest isolated yield (40.3%) but required intermediate transfer, increasing system complexity and risk of clogging (Scheme 3).

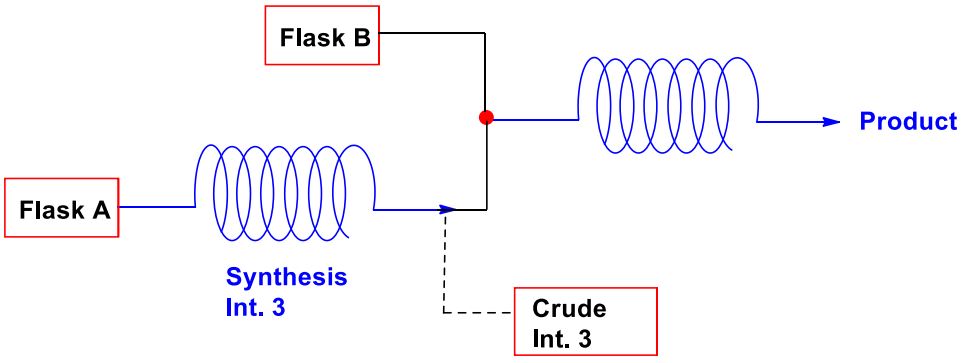

Scheme 3. Process A: Two-step configuration via Knoevenagel condensation (Intermediate 3 first).

Process **B** (Reverse Sequential: **4** + **5** → **1** + **2**): A reversed sequence, where carbanion formation preceded imine condensation, yielded comparable conversion and product yield (39.8%) but offered no operational advantage (Scheme 4).

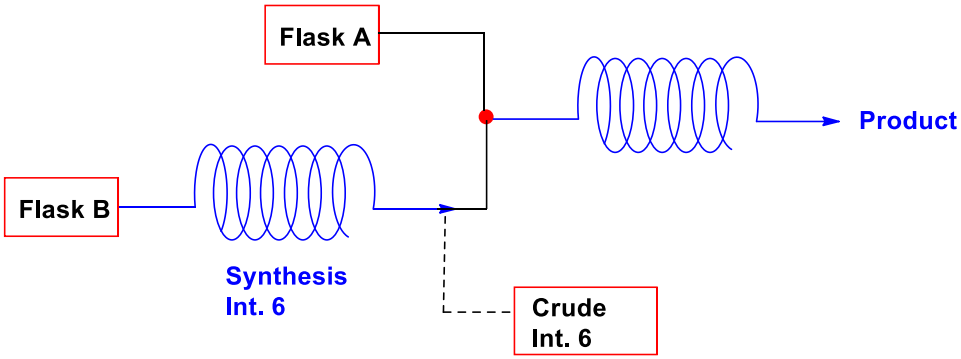

Scheme 4. Process B: Two-step configuration via Michael addition (Intermediate 6 first).

Process **C** (Simultaneous Addition): All five components were co-fed under identical flow rates and residence time. Despite a slightly lower yield (38.5%), this configuration eliminated stepwise transfer, reduced operational risk, and simplified microreactor setup (Scheme 5).

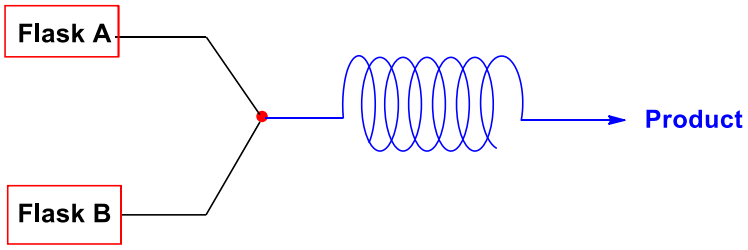

Scheme 5. Process C: One-step co-feeding configuration.

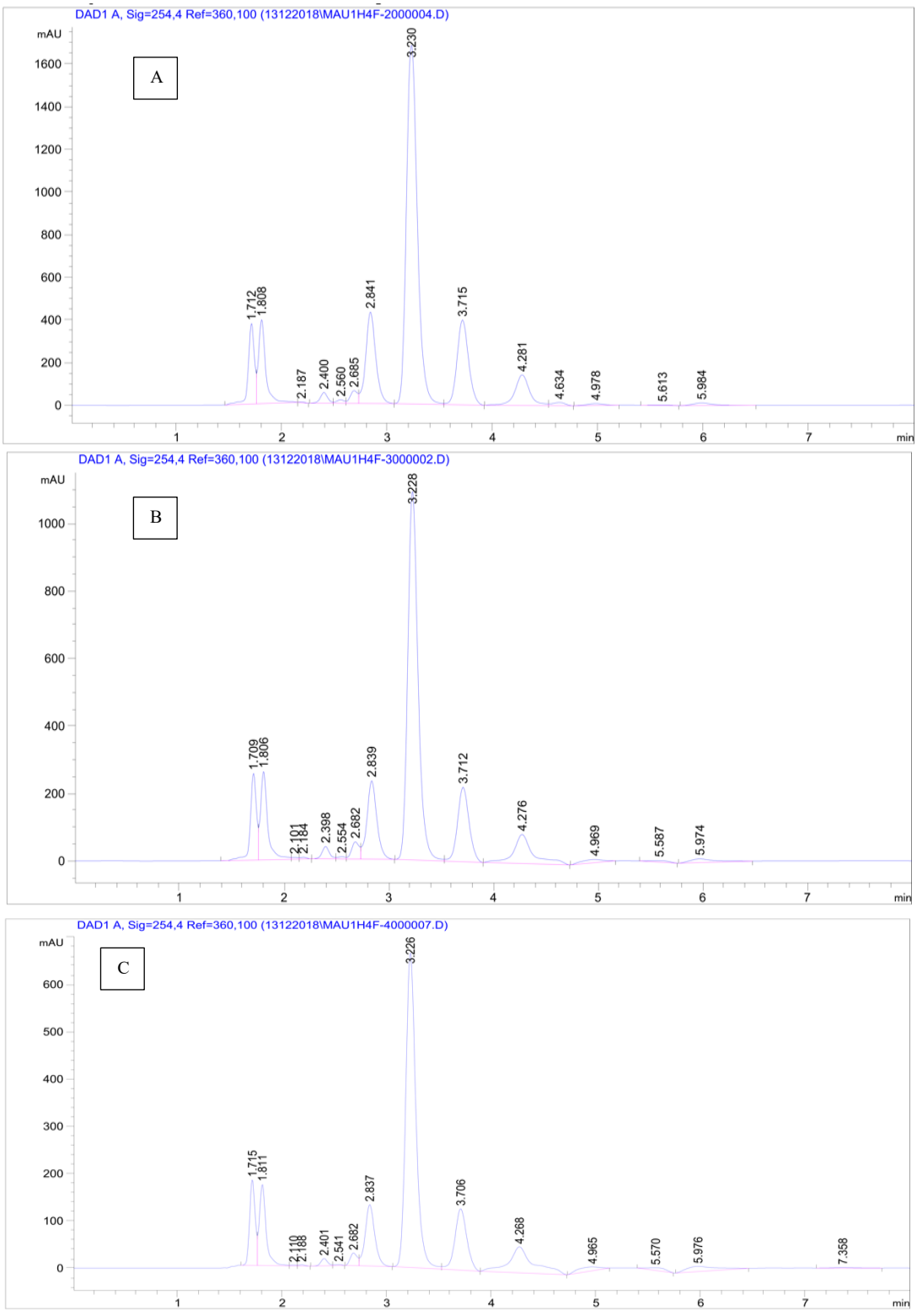

Figure 1. HPLC chromatogram of the reaction mixture from Process A (a, Peaks felodipine t_R 3.230 min); Process B (b, Peaks felodipine t_R 3.228 min); Process C (c, Peaks felodipine t_R 3.226 min).

As summarized in Table 1, all processes achieved full conversion. Given its operational simplicity and

comparable performance, Process C was selected for subsequent optimization.

Solvent screening. Solvent selection significantly affects this multicomponent reaction by influencing reactant solubility, reaction kinetics, and heat/mass transfer. Among the tested solvents, isopropanol (i-PrOH) gave the highest isolated yield of felodipine (52.9%) with excellent selectivity. Its moderate polarity and boiling point ensure sufficient solubilization of all organic substrates while maintaining favorable reaction kinetics. The HPLC chromatogram obtained under optimized *i*-PrOH conditions is displayed in Figure 2, showing a sharp peak for felodipine (tR 3.218 min).

In contrast, methanol and ethanol—despite being more polar—gave slightly lower yields (46.4% and 38.2%, respectively). Their higher water miscibility may disrupt the reaction equilibrium or promote hydrolysis of key intermediates. *n*-Butanol, with its higher boiling point and viscosity, impeded efficient mass transfer and increased by-product formation, resulting in a lower yield (26.4%). Water was the least effective solvent (5.7% yield), due to its poor solubility for organic components, which led to incomplete conversion (see Table 1 for detailed comparison).

All experiments were conducted under identical conditions: total flow rate 200 µL/min (100 µL/min per channel), 40 °C, acetic acid/pyridine catalyst system, and residence time of approximately 10 minutes.

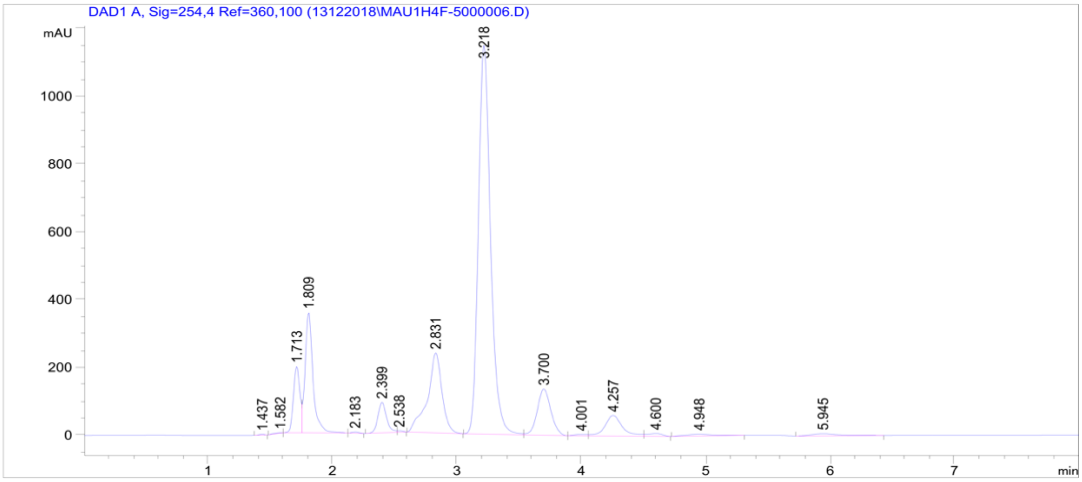

Figure 2. HPLC chromatogram of felodipine synthesis in i-PrOH under optimized conditions (Process C, 60 °C, NH_4OAc, AcOH/Pyr). Peaks: Felodipine (t_R = 3.218 min).

Temperature optimization. Reactions were conducted in isopropanol using acetic acid/pyridine as catalyst and ammonium acetate as nitrogen source. Flow rates were fixed at 100 µL/min per channel, with a residence time of 10 minutes. The temperature was varied from room temperature to 120 °C to assess its impact on conversion and product yield.

a) Room temperature to 40 °C: Incomplete conversion was observed, likely due to insufficient thermal activation energy for full multicomponent condensation.
b) 60 °C: Complete conversion and the highest felodipine yield (54.2%) were obtained, suggesting optimal activation without significant side reactions. The representative chromatogram at 60 °C is shown in Figure 3 (tR 3.199 min).
c) 80 °C to 120 °C: Although the reaction proceeded fully, the isolated yield gradually decreased (50.8% at

80 °C, 48.0% at 120 °C). This decline is likely due to thermal degradation or enhanced formation of by-products at elevated temperatures.

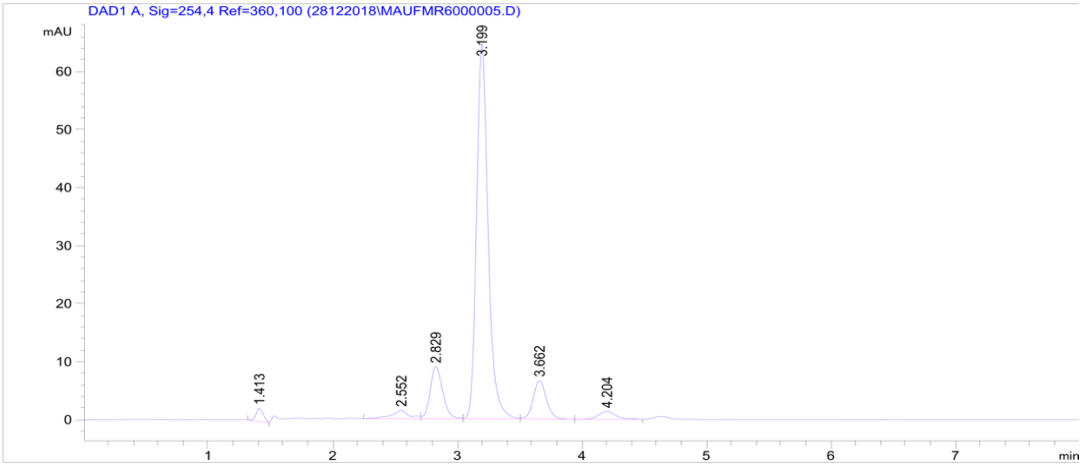

Figure 3. HPLC chromatogram of felodipine synthesis at 60 °C under optimized conditions (Process C, i-PrOH, NH_4OAc, AcOH/Pyr). Peaks: Felodipine (t_R = 3.199 min).

These results highlight a trade-off between reaction rate and product stability: higher temperatures promote faster reactions but may compromise product yield and selectivity. Therefore, 60 °C was selected as the optimal reaction temperature (see Table 1).

Nitrogen source screening. Various ammonium salts—including ammonium acetate (NH_4OAc), chloride (NH_4Cl), fluoride (NH_4F), sulfate $(NH_4)_2SO_4$, nitrate NH_4NO_3, carbonate $(NH_4)_2CO_3$, and hydroxide (NH_4OH)—were evaluated under identical continuous flow conditions (*i*-PrOH as solvent, acetic acid/pyridine catalyst, 60 °C, flow rate 100 µL/min per channel, residence time 10 min).

Among them, ammonium hydroxide (NH_4OH) yielded the highest felodipine yield (55.2%) with full conversion. However, due to its high volatility, corrosiveness, and strong basicity, NH_4OH posed operational challenges in the microreactor system, such as unstable dosing and potential damage to reactor components. Therefore, despite its high yield, NH_4OH was not selected for further development.

Instead, ammonium acetate (NH_4OAc) was chosen as the optimal nitrogen source, providing a high yield of 54.7% with good reproducibility and ease of handling. The HPLC chromatogram for felodipine obtained using ammonium acetate is shown in Figure 4, confirming high conversion and selectivity. Other salts such as NH_4Cl and NH_4F gave moderate yields (46.2% and 32.5%, respectively), while NH_4NO_3, $(NH_4)_2SO_4$, and $(NH_4)_2CO_3$ resulted in significantly lower yields (<50%) under the same conditions. Thus, the solubility, thermal stability, and reactivity of the ammonium salt play a critical role in determining reaction efficiency and product selectivity (see Table 1).

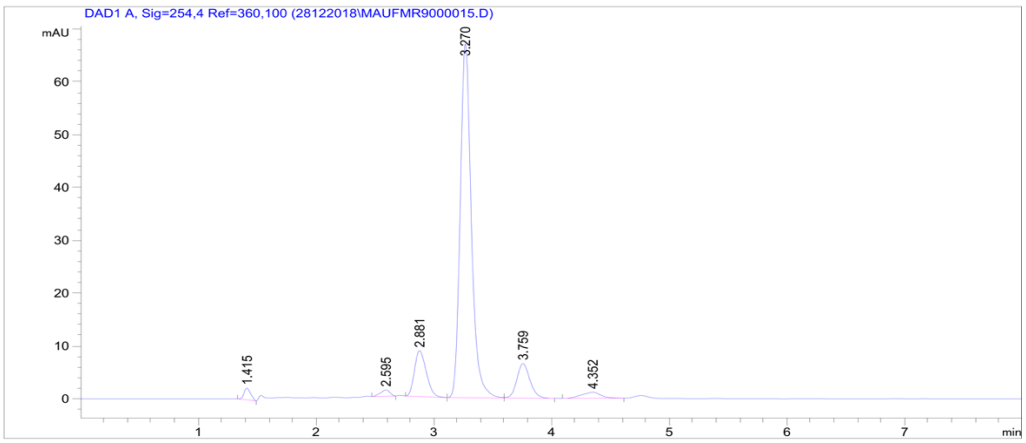

Figure 4. HPLC chromatogram of felodipine synthesis using ammonium acetate under optimized conditions (Process C, i-PrOH, 60°C, AcOH/Pyr). Peaks: Felodipine (t_R = 3.270 min).

Table 1. Optimization of Core Reaction Conditions for the Continuous Flow Synthesis of Felodipine

No.	Reaction Parameter	Condition/Entry	Conversion (%)	Felodipine Yield (%)
1	Reaction Process	A	100	40.3
		B	100	39.8
		C	100	38.5
2	Solvent	MeOH	100	46.4
		EtOH	100	38.2
		i-PrOH	100	52.9
		n-BuOH	100	26.4
		H_2O	64	5.7
3	Temperature	Room temp.	34	15.4
		40°C	100	43.7
		60°C	100	54.2
		80°C	100	50.8
		100°C	100	49.7
		120°C	100	48.0
4	Nitrogen Source	NH_4Cl	100	46.2
		NH_4F	92	32.5
		NH_4OAc	100	54.7
		$(NH_4)_2HSO_4$	84	28.4
		NH_4NO_3	100	49.8
		$(NH_4)_2CO_3$	100	48.0
		NH_4OH	100	55.2

2. Catalyst, stoichiometry, and flow optimization

Catalyst optimization. Catalyst choice is crucial for enabling the Hantzsch reaction under mild and efficient continuous flow conditions. A series of acid–base combinations[9-12] were screened to identify a system offering high yield, operational stability, and compatibility with flow parameters. Among the catalytic systems examined, acetic acid/piperidine afforded the highest yield of felodipine (59.2%), reflecting both superior catalytic efficiency and practical applicability, as clearly demonstrated by the chromatogram in Figure 5.

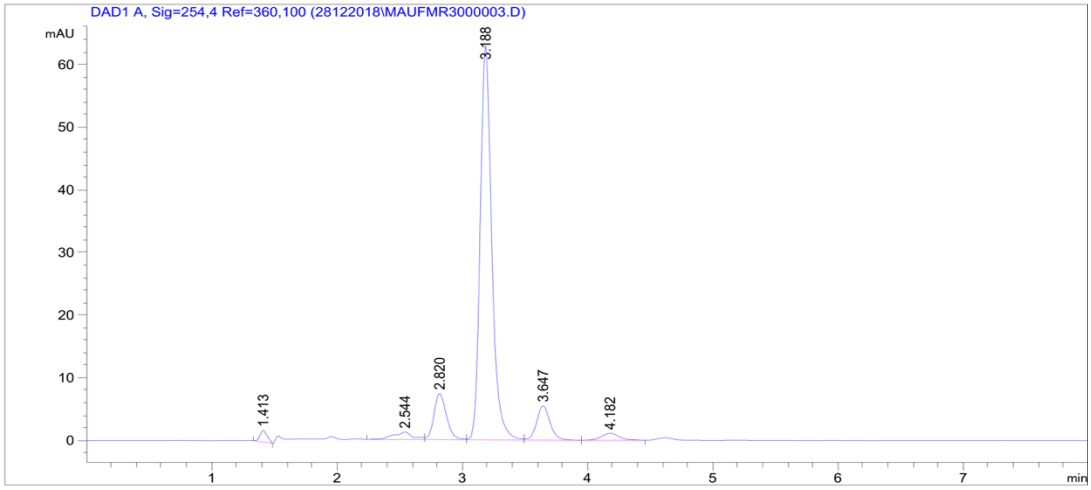

Figure 5. HPLC chromatogram of felodipine synthesis using acetic acid/piperidine under optimized conditions (Process C, i-PrOH, 60°C, NH_4OAc). Peaks: Felodipine (t_R = 3.188 min).

This combination outperformed other systems, including AcOH/L-proline (58.9%), AcOH/Et_3N (55.9%), AcOH/pyridine (54.2%), and AcOH/DIPEA (52.4%). Less effective systems such as Ph_3P and $PhB(OH)_2$ (<40%) suffered from low activity or poor compatibility under flow conditions (see Table 2).

Mechanistically, acetic acid activates carbonyl compounds, while piperidine promotes enamine formation and facilitates cyclization. This dual role enhances both the Knoevenagel and Hantzsch steps. Compared to advanced catalysts (e.g., ionic liquids,[21] TMSI,[22] $Yb(OTf)_3$,[23] iodine,[24] $Sc(OTf)_3$,[25] Ni nanoparticles,[26] Ru/Al_2O_3 nanocatalyst[27]), which often pose solubility, volatility, or cost issues in flow systems, piperidine is low-cost, stable, and well-suited for microreactors.

For these reasons, the AcOH/piperidine system was selected for all further experiments under standard flow conditions: isopropanol solvent, ammonium acetate, 60 °C, 100 µL/min/channel, and ~10 min residence time.

Flow rate optimization. Flow rate is a key parameter in continuous flow synthesis as it directly determines the residence time—the duration reactants spend in the reactor. This, in turn, affects both reaction efficiency (conversion and yield) and process throughput.

In this study, flow rates ranging from 100 to 600 µL/min per channel were systematically evaluated under identical conditions (isopropanol as solvent, NH_4OAc as nitrogen source, AcOH/piperidine as catalyst, at 60 °C). The results are summarized in Table 2.

a) At 100 µL/min, the reaction afforded the highest felodipine yield (61.0%), owing to the long residence time

that ensured complete condensation and cyclization. However, the low flow rate results in limited productivity, making it impractical for preparative or industrial applications. Doubling the rate to 200 µL/min slightly reduced the yield (59.1%) but doubled the throughput, offering better production efficiency.

b) At 400 µL/min, yield remained high (58.8%), while significantly increasing productivity. This rate provides an optimal balance between yield and scalability. The representative HPLC chromatogram obtained under these conditions is shown in Figure 6. Further increasing the flow to 600 µL/min led to a noticeable drop in yield (55.1%), likely due to insufficient residence time for complete reaction.

These observations illustrate a clear trade-off: while slower flow enhances conversion by prolonging reaction time, faster flow improves productivity but may sacrifice yield. Considering both factors, 400 µL/min per channel was selected as the optimal flow rate for subsequent experiments, offering high efficiency with scalable throughput under continuous flow conditions.

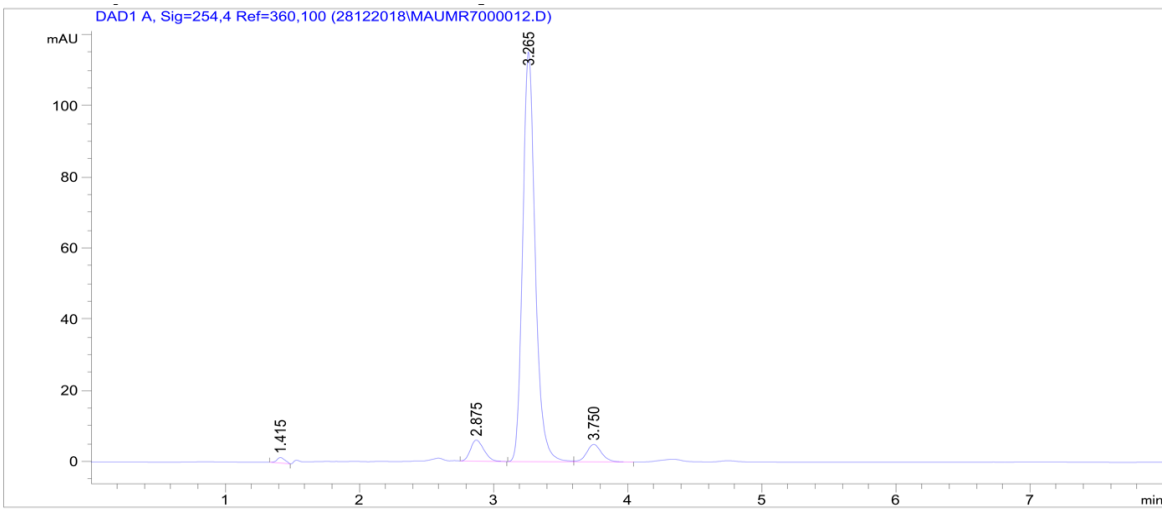

Figure 6. HPLC chromatogram of felodipine synthesis using a flow rate of 400 µl/min under optimized conditions (Process C, i-PrOH, 60°C, NH_4OAc, AcOH/Pip). Peaks: Felodipine (t_R = 3.265 min).

Molar ratio optimization. The total flow rate was maintained at 800 µL/min while varying individual flow rates of Flask A and Flask B to adjust the reagent molar ratio, corresponding to a residence time of approximately 10 minutes. A 1:1 flow ratio (400/400 µL/min) resulted in 58.6% yield. Adjusting to 364/436 µL/min (A:B ≈1:1.2) led to the highest yield (59.2%) and reduced by-product formation. The corresponding chromatogram is depicted in Figure 7, confirming selective formation of felodipine under these optimized stoichiometric conditions. Further deviation from this ratio reduced the yield and increased impurities, confirming the importance of fine-tuning stoichiometry in continuous flow processes (see Table 2).

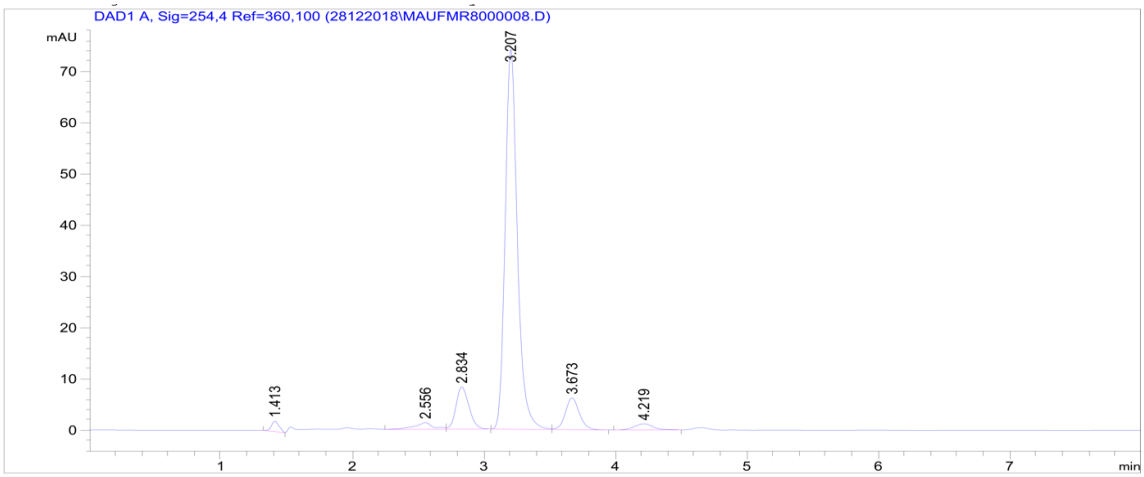

Figure 7. HPLC chromatogram of felodipine synthesis using flow rate ratio for channels A/B 364/436 under optimized conditions (Process C, i-PrOH, 60°C, NH_4OAc, AcOH/Pip, 400 µl/min). Peaks: Felodipine (t_R = 3.207 min).

Table 2. Catalyst, Stoichiometry, and Flow Optimization for the Continuous Flow Synthesis of Felodipine

No.	Reaction Parameter	Condition/Entry	Conv. (%)	Felodipine Yield (%)
5	Catalyst	AcOH/pyridine (1)	100	54.2
		AcOH/piperidine (2)	100	59.2
		AcOH/Et_3N (3)	100	55.9
		AcOH/DIPEA (4)	100	52.4
		AcOH/DMAP (5)	100	43.1
		AcOH/L-proline (6)	100	58.9
		Picolinic acid/piperidine (7)	100	50.2
		$ClCH_2COOH/PhCH_2NHMe$ (8)	100	43.1
		$PhB(OH)_2$ (9)	100	30.2
		Ph_3P (10)	100	32.5
6	Flow Rate	100 µL/min	100	61.0
		200 µL/min	100	59.1
		400 µL/min	100	58.8
		600 µL/min	100	55.1
7	Molar Ratio (Flow Rate A/B)	400/400	100	58.6
		364/436	100	59.2
		320/480	100	50.2
		267/533	100	42.5
		436/364	100	55.9
		480/320	100	45.3
		533/267	100	39.1

[1-8]Acid/amine: 2/0.5 (11.43 mmol/2.86 mmol); [9]10 mol% (0.57 mmol); [10]20 mol % (1.14 mmol)

In summary, optimal conditions for the continuous-flow synthesis of felodipine were established as follows: one-step co-feeding configuration (Process C), isopropanol as solvent, reaction temperature of 60 °C, ammonium acetate as nitrogen source, and acetic acid/piperidine (2:0.5) as catalyst system. A flow rate ratio of 364/436 μL·min^{-1} (Flask A/B, 1:1.2 molar ratio) afforded full conversion and an HPLC yield of 59.2%. After purification, felodipine was isolated in 40.1% yield with >98% purity. The difference between HPLC and isolated yield reflects cumulative material loss during multi-step purification.

In addition to yield and purity, continuous-flow synthesis presents further advantages over batch processing. The residence time is significantly shorter (≈10 min versus several hours in batch), which minimizes thermal stress and improves reproducibility. Operation in a microreactor coil enhances heat and mass transfer, preventing local overheating and enabling precise temperature control. The closed system setup ensures safer handling of volatile amines and acidic catalysts, reducing operator exposure. Moreover, the defined reactor geometry allows direct assessment of productivity and space–time yield, providing a transparent basis for scale-up.

Conclusions

We have developed an efficient and scalable continuous flow process for the synthesis of felodipine using a microreactor platform. Through systematic optimization of key parameters—including catalyst system, solvent, nitrogen source, and flow conditions—felodipine was obtained in 40.1% isolated yield with 98.4% purity in a short reaction time. Compared to conventional batch methods, this approach offers improved safety, reduced processing time, and better suitability for industrial scale-up. The study demonstrates that careful tuning of chemical and operational factors can significantly enhance the efficiency and selectivity of multicomponent reactions in flow.

Experimental Section

General. The Stuart SMP3 apparatus was employed to determine the melting point of the synthesized substances. The infrared spectrum was examined using a Nicolet Impact 410 spectrometer (Thermo Nicolet Corporation, USA) with KBr pellets. Nuclear magnetic resonance (NMR) spectra were obtained using an Avance AV500 Spectrometer manufactured by Bruker, a German-based company. The proton (1H) NMR spectra were recorded at a frequency of 500MHz, while the carbon-13 (^{13}C) NMR spectra were obtained at a frequency of 125MHz. The solvent used was deuterated dimethyl sulfoxide (DMSO-d_6), and tetramethylsilane (TMS) was used as the internal standard.

The continuous flow reactions were carried out using an Easy-MedChem™ E-Series flow chemistry system (Vapourtec Ltd., UK) equipped with a PFA micoreactor coil (internal diameter 1.0 mm, reactor volume 10 mL; Vapourtec part no. 50-1011, length ≈ 12.7 m). Solutions were introduced via a dual-syringe pumping module integrated with the system. Based on the total flow rate of 0.80 mL·min^{-1} and the effective internal volume of the system, the measured residence time was 10.0 min. This value is slightly shorter than the theoretical residence time of 12.5 min expected for a 10 mL coil, likely due to dead volume contributions and system

configuration. During a 6.15 h steady-state production run, 11.0 g of felodipine (≈30.4 mmol) was isolated (40.1% yield), corresponding to a productivity of 4.94 mmol·h^{-1} (≈1.79 g·h^{-1}) and a space–time yield (STY) of ≈179 g·L^{-1}·h^{-1}.

Chemical reagents with high purity were bought from Merck Chemical Company. All reagents were of a grade for organic synthesis. The felodipine standard is provided by the National Institute of Drug Quality Control (Viet Nam). Two feed solutions (Flask A and Flask B) were prepared and pumped through the PFA tubing into the heated reactor. Flask compositions and flow conditions were systematically varied to optimize the synthesis of felodipine. The optimized conditions (see below) afforded felodipine in 40.1% yield (98.4% purity). The quantity of felodipine in the product mixture was determined by HPLC (Agilent 1260 Series, USA) under the following conditions: injection volume 5 µL; flow rate 1.0 mL/min; mobile phase consisting of methanol/phosphate buffer (85:15, v/v, pH 3.0); column: ZORBAX XDB-C18; detection: DAD at 254 nm.[28]

A stock solution of felodipine was prepared by accurately weighing 0.05 g of felodipine reference standard and dissolving it in 10 mL of mobile phase, which consisted of 85% phosphate buffer and 15% methanol. This stock solution had a concentration of 5 mg/mL.

From this stock solution, a series of standard working solutions were prepared by appropriate dilution to obtain final concentrations of 0.2, 0.4, 0.6, 0.8, and 1.0 mg/mL. Each standard solution was analyzed under the same chromatographic conditions, and the corresponding peak areas were recorded.

A calibration curve was then constructed by plotting the peak area against the concentration of felodipine (mg/mL). The resulting linear regression equation was: y = 7076.9x + 87.698, with a correlation coefficient R^2 = 0.9997, indicating excellent linearity across the tested concentration range (see Figure 8).

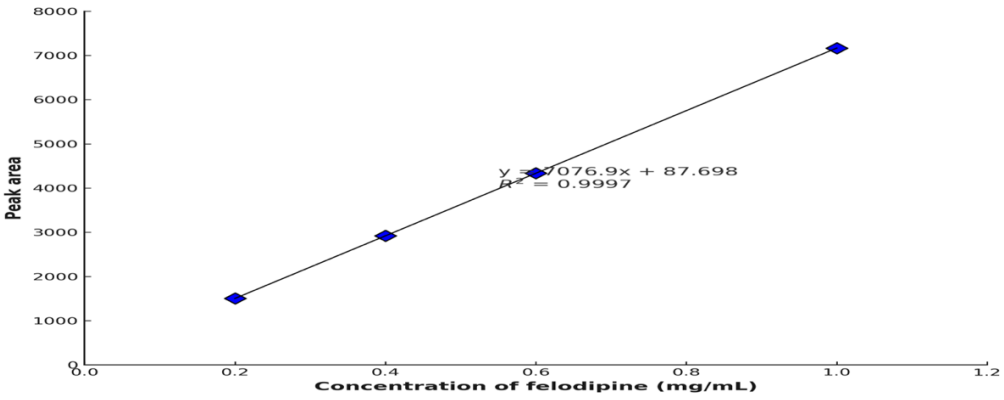

Figure 8. Calibration curve for quantification of felodipine.

The HPLC chromatogram of felodipine standard (5 mg/mL) shows a sharp, symmetrical peak at 2.865 min, detected at 254 nm using a DAD. The absence of interfering peaks near the retention time confirms the method's specificity and supports the use of this standard in calibration curve construction (see Figure 9).

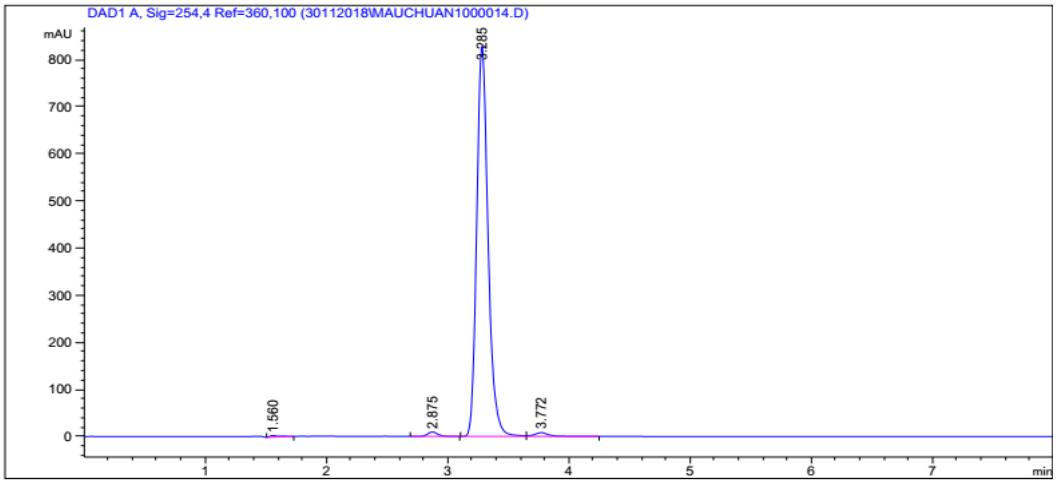

Figure 9. HPLC chromatogram of felodipine standard solution.

$$\text{Amount of Felodipine (mg)} = \frac{\text{Speak} - 87.698}{7076.9} \times \text{Dilution volume (mL)}$$

$$\text{Yield (\%)} = \frac{\text{Amount of Felodipine (mg)}}{\text{Theoretical amount (mg)}} \times 100$$

i. Reaction process design

Preparation of Feed Solutions:

a) Flask A: A solution of **2** (1.00 g, 5.7 mmol), **1** (0.66 g, 5.7 mmol), pyridine (0.56 mL, 6.95 mmol), and acetic acid (0.32 mL, 5.59 mmol) was prepared in 15 mL of ethanol.

b) Flask B: A solution of **4** (0.74 g, 5.7 mmol) and **5** (0.53 g, 6.88 mmol) was prepared in 15 mL of ethanol.

Process Optimization Strategy: To evaluate the effect of reagent feeding mode on reaction efficiency, three process configurations were investigated under identical conditions (40 °C, 100 µL/min per channel, residence time 10 min):

a) Process A: A two-step configuration in which intermediate **3** was first generated from Flask A via Knoevenagel condensation in channel A. The resulting output stream was subsequently introduced, without isolation, into channel B, where it reacted with the contents of Flask B to yield the final product

b) Process B: A two-step route wherein intermediate **6** was first formed from Flask B via Michael-type addition in channel B. The output stream was then directed to channel A, where it was combined with the contents of Flask A for the second step.

c) Process C: A one-step co-feeding configuration where solutions from both Flask A and Flask B were introduced simultaneously into a single microreactor through separate channels. All components reacted in situ under continuous flow conditions.

ii. Solvent screening

Methanol, ethanol, isopropanol, n-butanol, and water (15 mL) were tested under identical conditions: 100 µL/min per channel, reactor temperature 40 °C, acetic acid/pyridine catalyst, and residence time of approximately 10 minutes.

iii. Temperature optimization

Reactions were performed using isopropanol, acetic acid/pyridine, and ammonium acetate, with flow rates of 100 µL/min per channel and a residence time 10 minutes. The temperature range studied was from room

temperature to 120 °C.

iv. Nitrogen source screening

Ammonium acetate, ammonium chloride, ammonium fluoride, ammonium sulfate, ammonium nitrate, ammonium carbonate, and ammonium hydroxide were tested under identical reaction conditions.

v. Catalyst screening

Catalyst systems consisting of acetic acid with various amines (pyridine, piperidine, triethylamine, DIPEA, DMAP, L-proline,…) were evaluated using isopropanol, ammonium acetate, and a reactor temperature of 60 °C, with flow rates of 100 µL/min per channel and a residence time 10 minutes.

vi. Flow rate optimization

Flow rates ranging from 100 to 600 µL/min per channel were applied under constant conditions using isopropanol, ammonium acetate, acetic acid/piperidine, and a reactor temperature of 60 °C.

vii. Molar ratio adjustment

The total flow rate was maintained at 800 µL/min while varying individual flow rates of Flask A and Flask B to adjust the reagent molar ratio, corresponding to a residence time 10 minutes.

Continuous flow synthesis of Felodipine (optimized conditions)

A solution of **2** (2,3-dichlorobenzaldehyde, 10.0 g, 57.0 mmol), **1** (methyl acetoacetate, 6.63 g, 57.0 mmol), piperidine (5.6 mL, 56.7 mmol), and acetic acid (3.27 mL, 56.7 mmol) in isopropanol (150 mL) was prepared as Flask A. Separately, a solution of **4** (ethyl acetoacetate, 7.44 g, 57.0 mmol) and **5** (ammonium acetate, 5.29 g, 68.8 mmol) in isopropanol (150 mL) was prepared as Flask B. Both solutions were freshly prepared immediately before use to ensure complete dissolution and to avoid any premature reaction prior to introduction into the microreactor.

The solutions were delivered using a dual-syringe pump into a PFA microreactor coil. The flow rates were set at 364 µL/min for Flask A and 436 µL/min for Flask B. The microreactor coil was thermostated in a water bath maintained at 60 °C. The reaction was run under steady-state conditions for 6.15 h.

After completion, the outflow was collected and concentrated under reduced pressure using a rotary evaporator to remove isopropanol. The resulting crude residue was dissolved in 50 mL of dichloromethane (DCM) and washed with 50 mL of 1 M $NaHCO_3$ solution. The organic phase was separated and evaporated to dryness.

The residue was redissolved in 30 mL of ethanol and stirred at 70 °C for 10 min. Subsequently, 60 mL of 2 M HCl was added, and the mixture was stirred at 70 °C until TLC indicated complete conversion of felodipine to its hydrochloride salt. Ethanol was evaporated, and the residue was extracted with ethyl acetate. The aqueous phase was neutralized to pH 7 with solid $NaHCO_3$ and extracted with DCM (3 × 30 mL). The combined DCM layers were dried under reduced pressure.

The resulting residue was dissolved in 30 mL of toluene and stirred at 70 °C until a clear solution was obtained. Then, 30 mL of *n*-hexane was slowly added, and the mixture was cooled at 5 °C for 6 h. The precipitated solid was collected by vacuum filtration and washed with 50 mL of pre-cooled (–10 °C) 1:5 toluene/n-hexane. The product was dried under vacuum at 40 °C.

The filtrate was reprocessed by dissolving in 20 mL of toluene at 70 °C, followed by slow addition of 20 mL of n-hexane. Crystallization was allowed to proceed under the same cooling conditions. This recrystallization cycle was repeated three times (each with 10 mL toluene and 10 mL n-hexane).

This multi-step purification was necessary due to the co-formation of side products and colored impurities typical of Hantzsch condensations. Extraction with dichloromethane ensured efficient phase separation, while salt formation and successive recrystallizations progressively improved purity from ~90% (after the first

crystallization) to >98% (final product, confirmed by HPLC). These additional purification steps inevitably reduced the isolated yield compared with the HPLC yield. After purification, felodipine was obtained as a white crystalline solid (11,0 g, 40.1% isolated yield, 98.4% purity, 100% conversion). Physical, IR, NMR, and HRMS spectra data of felodipine are reported as follows: mp 145-146 °C. IR(KBr, cm^{-1}): 3371 (NH), 1699 (CO), 1496 (C=C); 1205, 1098 (C-O). ^{1}H NMR(δ ppm, DMSO-d_6): 7.29 (1H, dd, *J* 8.0, 1.5 Hz, Ar-H), 7.24 (1H, dd, *J* 8.0, 1.5 Hz, Ar-H), 7.06 (1H, t, *J* 8.0, 7.5 Hz, Ar-H), 5.77 (1H, s, NH), 5.47 (1H, s, 1,4-DHP-H), 4.07 (2H, q, *J* 7.5 Hz, $COO\underline{CH_2}CH_3$), 3.60 (3H, s, $-COO\underline{CH_3}$), 2.30 (3H, s, 1,4-DHP-CH_3), 2.29 (3H, s, 1,4-DHP-CH_3), 1.18 (3H, t, *J* 7.0 Hz, $COOCH_2\underline{CH_3}$). ^{13}C NMR (δ, DMSO-d_6): 167.9, 167.4, 148.1, 144.2, 144.1, 132.8, 131.0, 129.7, 128.2, 127.0, 104.9, 103.5, 59.8, 50.8, 38.6, 19.5, 19.4, 14.3. HRMS (EI) *m/z*: $[M]^{+\bullet}$ calcd for $C_{18}H_{19}Cl_2NO_4$ = 362.0618; found = 362.0677 (100).

Supplementary Material

Copies of NMR and IR spectra associated with this paper are provided in the accompanying Supplementary Material.

References

1. Chen, X.; Ji, Z.L.; Chen, Y.Z. *Nucleic Acids Res.* **2002**, *30*(1), 412–415. https://doi.org/10.1093/nar/30.1.412
2. Furukawa, T.; Yamakawa, T.; Midera, T.; Sagawa, T.; Mori, Y.; Nukada, T. *J. Pharmacol. Exp. Ther.* **1999**, *291*(2), 464–473. https://pubmed.ncbi.nlm.nih.gov/10525060/
3. Kim, J.; Jeon, S.G.; Jeong, H.R.; Park, H.; Kim, J.I.; Hoe, H.S. *Int. J. Mol. Sci.* **2022**, *23*(21), 13606. https://doi.org/10.3390/ijms232113606
4. Espinosa-Parrilla, J.F.; Martinez-Moreno, M.; Gasull, X.; Mahy, N.; Rodriguez, M. *J. Mol. Cell. Neurosci.* **2015**, *64*, 104–115. https://doi.org/10.1016/j.mcn.2014.12.004
5. Sinnegger-Brauns, M.J.; Huber, I.G.; Koschak, A.; Wild, C.; Obermair, G.J.; Einzinger, U.; Hoda, J.C.; Sartori, S.B.; Striessnig, J. *Mol. Pharmacol.* **2009**, *75*(2), 407–414. https://doi.org/10.1124/mol.108.049981
6. Peterson, B.Z.; Catterall, W.A. *Mol. Pharmacol.* **2006**, *70*(2), 667–675. https://doi.org/10.1124/mol.105.020644
7. Cohen, C.J.; Spires, S.; Van Skiver, D. *J. Gen. Physiol.* **1992**, *100(*4), 703–728. https://doi.org/10.1085/jgp.100.4.703
8. Lamers, J.M.; Cysouw, K.J.; Verdouw, P.D. *Biochem. Pharmacol.* **1985**, *34(*21), 3837–3843. https://doi.org/10.1016/0006-2952(85)90432-0
9. Desai, R. et al. US Patent 5,977,369. 1999. https://patents.google.com/patent/US5977369A/en
10. Auerbach, J. et al. US Patent 5,310,917. 1994. https://patents.google.com/patent/US5310917A/en

11. Cascio, G.; Castelli, E. Manghisi, E. WO98/07698. 1998. https://patents.google.com/patent/WO1998007698A1/en
12. Gustavsson, A. US Patent 5,942,624. 1999. https://patents.google.com/patent/US5942624A/en
13. Vu, M.T.; Le, T.H.N.; Nguyen, N.T.; Nguyen, Q.T.; Doan, D.T. *Pharm. J.* **2018**, *58*(510), 75–77. (in Vietnamese). https://vjol.info.vn/index.php/tcdh/issue/view/3811
14. Socal, M.P.; Sharfstein, J.M.; Greene, J.A. *Am. J. Public Health*. **2021**, *111*, 635–639. https://doi.org/10.2105/AJPH.2020.306138
15. Lee, S.L.; O'Connor, T.F.; Yang, X.; Cruz, C.N.; Chatterjee, S.; Madurawe, R.D.; Moore, C.M.V.; Yu, L.X.; Woodcock, J. *J. Pharm. Innov.* **2015**, *10,* 191–199. https://doi.org/10.1007/s12247-015-9215-8
16. Plutschack, M.B.; Pieber, B.; Gilmore, K.; Seeberger, P.H. *Chem. Rev.* **2017**, *117,* 11796–11893. https://doi.org/10.1021/acs.chemrev.7b00183
17. Baumann, M.; Moody, T.S.; Smyth, M.; Wharry, S. *Eur. J. Org. Chem.* **2020**, *2020*, 7398–7406. https://doi.org/10.1002/ejoc.202001278
18. Fülöp, Z.; Szemesi, P.; Bana, P.; Éles, J.; Greiner, I. *React. Chem. Eng.* **2020**, *5*, 1527–1555. https://doi.org/10.1039/D0RE00273A
19. Baumann M., Moody TS., Smyth M., Wharry S. *Org. Process Res. Dev.,* **2020**, *24*, 1802–1813. https://doi.org/10.1021/acs.oprd.9b00524
20. Hantzsch, A. *Chem. Ber.*, **1881**, *14*(2), 1637–1638. https://doi.org/10.1002/cber.18810140214
21. Sridhar, R.; Perumal, P.T. *Tetrahedron* **2005**, *61*, 2465–2470. https://doi.org/10.1016/j.tet.2005.01.008
22. Sabitha, G.S.; Kiran, K.R.; Ch, S.R.; Yadav, A.S. *Tetrahedron Lett.* **2003**, *44*, 4129–4131. https://doi.org/10.1016/S0040-4039(03)00813-X
23. Wang, L.M.; Scheng, J.; Zhang, L.; Han, J.W.; Fan, Z.Y.; Tian, H.; Qian, C.T. *Tetrahedron* **2005**, *61*, 1539–1543. https://doi.org/10.1016/j.tet.2004.11.079
24. Ko, S.; Sastry, M.N.V.; Lin, C. Yao, C.F. *Tetrahedron Lett.* **2005**, *46*(34), 5771–5774. https://doi.org/10.1016/j.tetlet.2005.05.148
25. Donelson, J.L.; Gibbs, R.A.; De, S.K. *J. Mol. Catal. A Chem.* **2006**, *256*, 309–311. https://doi.org/10.1016/j.molcata.2006.03.079
26. Sapkal, S.B.; Shelke, K.F.; Shingate, B.B.; Shingare, M.S. *Tetrahedron Lett.* **2009**, *50*(15), 1754–1756. https://doi.org/10.1016/j.tetlet.2009.01.140
27. Saadatjou, N.; Jafari, A.; Sahebdelfar, A. *Iran. J. Chem. Chem. Eng.* **2015**, *34*(1), 1–9. https://doi.org/10.30492/IJCCE.2015.12613
28. Le, T.H.N.; Nguyen, M.H.; Nguyen, N.T.; Nguyen, Q.T.; Vu, M.T. *Pharm. J.* **2019**, *59*(516), 46–49. (in Vietnamese). https://vjol.info.vn/index.php/tcdh/issue/view/3894